Available online at www.sciencedirect.com
SCIENCE DIRECT®
Marine Geology 201 (2003) 67–79
MARINE GEOLOGY
INTERNATIONAL JOURNAL OF MARINE GEOLOGY, GEOCHEMISTRY AND GEOPHYSICS
www.elsevier.com/locate/margeo

Toward establishing a maritime proxy record of the East Asian summer monsoons for the late Quaternary

Kuo-Yen Wei [a,*], Tzu-Chien Chiu [a,b], Yue-Gau Chen [a]

[a] *Institute of Geosciences, National Taiwan University, P.O.Box 13-318, Taipei, Taiwan*
[b] *Lamont–Doherty Earth Observatory, Palisades, NY 10964, USA*

Accepted 19 June 2003

Abstract

An astronomically tuned late Quaternary planktic foraminiferal $\delta^{18}O$ record of Site MD972142 (12°41.33′N, 119°27.90′E; 1557 m water depth) in the southeastern South China Sea was established. The difference in $\delta^{18}O$ between MD972142 and ODP792 of the Sulu Sea is regarded as a maritime proxy of the summer monsoon intensity over the South China Sea and Southeast Asia. The profile of this maritime proxy matches well with the summer monsoon index obtained from the terrestrial record of Louchuan, central Chinese Loess Plateau. The amplified planktic $\delta^{18}O$ signals of the South China Sea relative to the Sulu Sea record are partly caused by the changing intensities of the East Asian Monsoons at the glacial–interglacial time-scale throughout the late Quaternary.

1. Introduction

In studying the Asian summer monsoon as a major component of the global climate system, various indices have been developed to quantify its intensity for modern monsoon climatology, such as monsoon rainfall over India, the vertical shear in the zonal wind between 850 and 200 hPa over the monsoon region (the M1* index of Webster and Yang, 1992). In paleoclimatological studies, researchers have also established various proxies to gauge the intensity of paleomonsoons. For instance, the magnetic susceptibility in the paleosol–loess sequences of the Chinese Loess Plateau has been used as a good proxy of summer monsoon (An et al., 1990, 1991; Verosub et al., 1993; Porter et al., 2001), whereas the loess grain size has been considered as an index for the winter monsoon (Ding et al., 1995). For paleoceanographic records, the relative abundance of *Globigerina bulloides*, a planktic foraminifer affiliated with upwelling induced by the southwesterly summer monsoon in the NW Indian Ocean, has demonstrated to be a good proxy for the marine records of the Indian Ocean (Prell et al., 1990). Nevertheless, establishing a robust proxy of the East Asian summer paleomonsoon intensity from sedimentary records in the South China Sea (SCS) has been posited as a major challenge.

Several proxies have been proposed. For instance, the deviation of the $\delta^{18}O$ signal of the mixed-layer planktic foraminifer *Globigerinoides ruber* from the main pattern of glacial–interglacial

* Corresponding author. Tel.: +886-2-23691143; Fax: +886-2-23636095.
E-mail address: weiky@ms.cc.ntu.edu.tw (K.-Y. Wei).

0025-3227/03/$ – see front matter © 2003 Elsevier B.V. All rights reserved.
doi:10.1016/S0025-3227(03)00209-3

fluctuation was considered as an index of summer monsoon intensity, as inferred from its covariance with reduced sea-surface salinity and increased input of fluvial clay (P. Wang et al., 1999). Increases in herbaceous pollen and charcoal from the same marine sedimentary sequence of Core 17940 in the northern SCS during the glacial also has been regarded indicating aridity and hence a sign of weakened summer monsoon (Sun and Li, 1999). More recently, Jian et al. (2001) strategically selected two sites from the summer and winter upwelling areas in the SCS and used four upwelling proxies (benthic foraminiferal flux, organic carbon flux, relative abundance of *Uvigerina peregrina*, estimated depth of thermocline) to infer indirectly the strength of summer and winter monsoons.

In this paper, we propose that the difference in $\delta^{18}O$ of the planktic foraminifer *Globigerinoides ruber* between the SCS and the Sulu Sea can serve as a proxy of the intensity of summer monsoon over Southeast Asia for the late Quaternary. Such deviation in $\delta^{18}O$ of the SCS from the Sulu Sea record is considered to be related to the intensity of precipitation which, in turn, was mainly enhanced by summer monsoons in the SCS and surrounding lands. We will first present a newly obtained astronomically tuned timescale of planktic $\delta^{18}O$ for the past 870 kyr from Site MD972142, eastern SCS (Fig. 1), and then compare it with a comparable record of ODP Site 769 from the Sulu Sea (Linsley and Dunbar, 1994; Linsley, 1996). In interpreting the difference between these two records, we will present our rationale in using it as a proxy of the summer monsoon intensity over the vast area of the Southeast Asia for the late Quaternary. Temporal variations of this summer monsoon index are then compared with the classical magnetic susceptibility record at Louchuan in the central Chinese Loess Plateau (Lu et al., 1999; Heslop et al., 2000). The striking similarity in these two proximal records of summer monsoons appears to support our interpretation.

2. Site MD972142 and its oceanographic setting

During the 1997 IMAGES-III-IPHIS Cruise (Chen and Beaufort, 1998), Core MD972142 (12°41.33′N, 119°27.90′E) (Fig. 1) was raised from the continental slope off Palawan Island at a water depth of 1557 m. The seafloor at this site is much shallower than the calcite lysocline (~2500 m; Rottman, 1979) of the SCS so that calcareous foraminifera and nannofossils are well preserved. Because of the moderately low sedimentation rates at this site and long core recovery in length (35.91 m), a record with sufficiently high resolution, covering the whole Brunhes magnetochron is preserved in this core (Lee, 2000).

The transportation of salt in the basin was mainly driven by the inflow of Western Philippine Sea (WPS) waters entering from the Luzon Strait (between Taiwan and Luzon), and meanwhile the waters in the basin are diluted by river runoff from the surrounding lands (Wyrtki, 1961). Summer sea-surface salinities range between 32.8 and 33.6‰, but the north–south gradient in salinity in the SCS increases during the winter with a branch of warm, saline Kuroshio enters into the SCS through the Luzon Strait (Shaw, 1989, 1991), mixing with colder waters from the north via the Taiwan Strait. These two surface water masses combine and flow southward along the coast of Indochina Peninsula and result in a counterclockwise circulation. The salinities during winter increase generally, with a wide range from 33.2 to 34.4‰ (Levitus and Boyer, 1994). Changes in the freshwater budget have had a great impact on the circulation. According to Wytrki (1961), the saline waters (>34.9‰) which enter the SCS as a subsurface flow are mainly from the North Subtropical Lower Water while the less saline waters (34.2~34.3‰) in the upper part are from the North Pacific Intermediate Water. The difference between the S_{max} and S_{min} in the vertical profile decreases as the waters flow southward into the basin due to vertical mixing. On the other hand, the salinity of the surface water shows also a southward decreasing trend. The gradient along the north–south transect is controlled partly by the dilution effect of freshwater input from the Indochina Peninsula. The SCS water flows northwards out through the Luzon Strait along the coast of Luzon and enters to the WPS (Wyrtki,

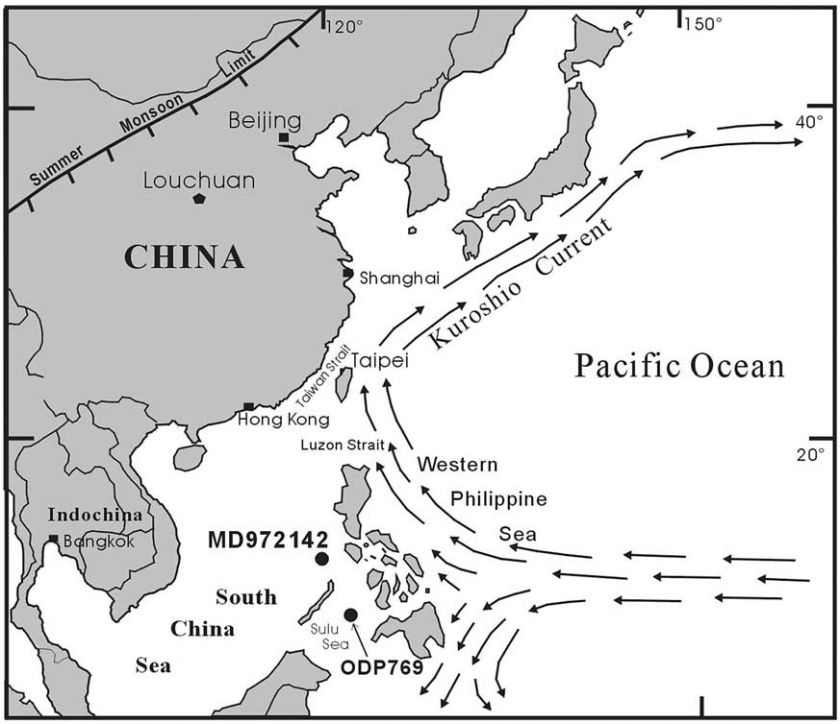

Fig. 1. Location map of East Asia and Pacific showing locations of the three sites examined: MD972142 in the eastern SCS, ODP769 in the Sulu Sea, and Louchuan on the central Chinese Loess Plateau. The ticked line marks the current northwestern limit of the summer monsoon.

1961; Nitani, 1972; Gong et al., 1993; Chen and Huang, 1996). The SCS water flows out mainly at the intermediate depth of 350–1350 m, and joins the Kuroshio, entrained as the left-hand part of the Kuroshio flowing northward (Chen and Huang, 1996). The salinity range of the outflow water is between 34.45 and 34.6‰ (Chen and Huang, 1996). It is obvious that precipitation and thus freshwater influx to the basin plays an important role in regulating the salt budget of the SCS.

For the late Quaternary, another major factor that affects paleoceanographic conditions is the large-amplitude sea-level fluctuation associated with global ice-volume changes. There is a large extent of continental shelves distributed in the western Pacific marginal seas, and therefore, glacial-induced sea-level drop shrank the area of marginal seas significantly (P. Wang, 1999). In the SCS for example, during the glacial periods, large areas of the continental shelves (such as the Sunda Shelf) were exposed, closing the gateways between the southwestern SCS and Indian Ocean. Shrinkage of basin area and enhanced northeastern monsoon would both tend to lower the moisture flux conveyed inland, consequently aridity in mainland China became enhanced during glacial periods (P. Wang, 1999).

3. Materials and methods

The sedimentary sequence at Site MD972142 consists dominantly of fine-grained hemipelagic sediments intercalated with more than a dozen discrete tephra layers. The thickness of the individual tephra layers ranges from 0.5 to 10 cm; they are on average thicker than 1 cm (Wei et al., 1998b).

For stable oxygen and carbon isotope analyses,

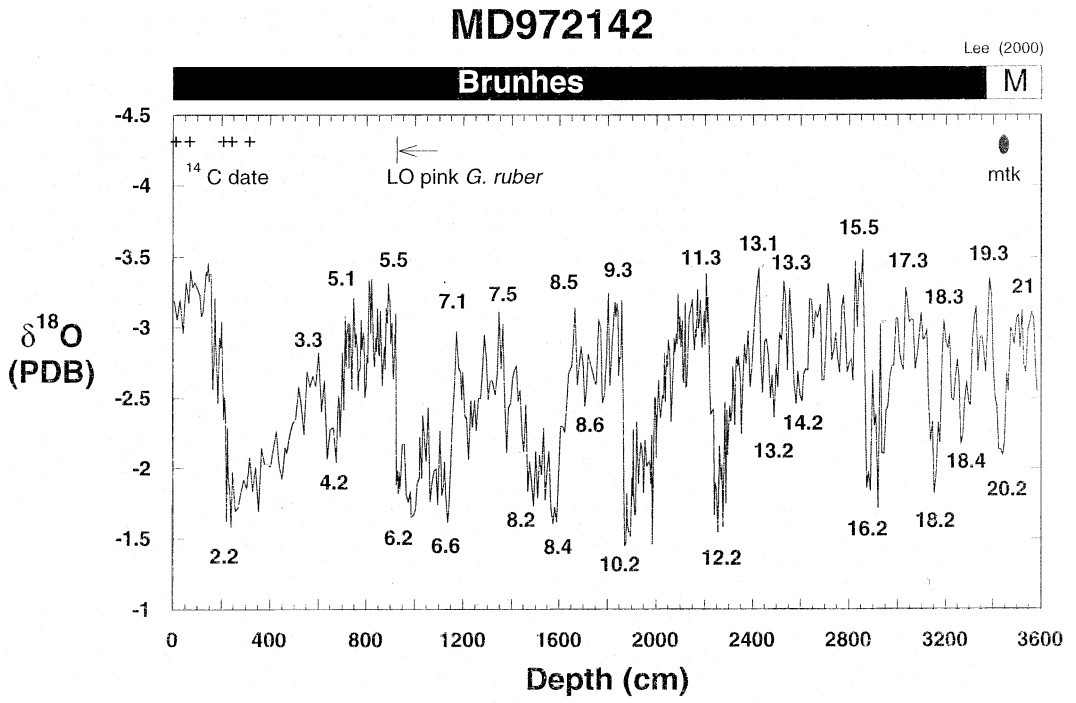

Fig. 2. Oxygen isotope profile of *Globigerinoides ruber*, Core MD972142. The depth scale is cm in subdepth below the seafloor. Numbers mark the marine isotope stages correlated to the low-latitude stack of Bassinot et al. (1994). Shown on the top are the magnetostratigraphy from Lee (2000), the last occurrence datum of pink *G. ruber*, and the position of the Australasian microtektite layer (marked as mtk) (Lee and Wei, 2000).

samples were taken every 4–12 cm as to obtain a temporal resolution of at least 1 sample per 2000 years. Specimens of planktic foraminifera *Globigerinoides ruber* s.s (white) in the 250~300-μm size fraction were picked from sieved sediments for isotopic analysis. Confining the size of foraminiferal specimens in such a narrow range results in having picked specimens in the same ontogenetic stage (Brummer et al., 1987; Wei et al., 1992), thus excluding vital effects in stable isotope signals. About eight specimens of *Globigerinoides ruber* were immersed in CH_3OH and subjected to ultrasonic vibration for 6 s three times and then immersed in NaOCl for 24 h. After being cleaned by deionized water five times and dried, the specimens were reacted with 100% H_3PO_4 at 70°C to generate CO_2 gas in a Kiel Device; then the CO_2 gas was sent into the Finnigan MAT Delta^{plus} mass spectrometer to determine its $\delta^{18}O$ and $\delta^{13}C$ values. All $\delta^{18}O$ and $\delta^{13}C$ values were converted to the Pee Dee Belemnite scale. The NBS-19 was used as calibration standard ($\delta^{18}O = -2.20‰$, $\delta^{13}C = +1.95‰$). External precision of the measurements was better than 0.08‰ for $\delta^{18}O$ and 0.04‰ for $\delta^{13}C$, as shown by routine repeatedly analysis of the internal laboratory standard.

In all 250 specimens of *Globigerinoides sacculifer* (>300-μm size fraction) picked from five depths in the uppermost part of Core MD972142 were sent to Rafter Radiocarbon Laboratory, Institute of Geological and Nuclear Sciences, New Zealand, for ^{14}C accelerator mass spectrometry (AMS) dating. The last appearance datum (LA) of pink *Globigerinoides ruber* at about 120 ka has been considered a good biostratigraphic marker in the western Pacific (Thompson et al., 1979). Lee et al. (1999) reported recently that the age of this datum is 127 ka at Site MD972151 in the southwest SCS. The last occurrence of pink *G. ruber* at Site MD972142 was found at a subdepth of 910 cm.

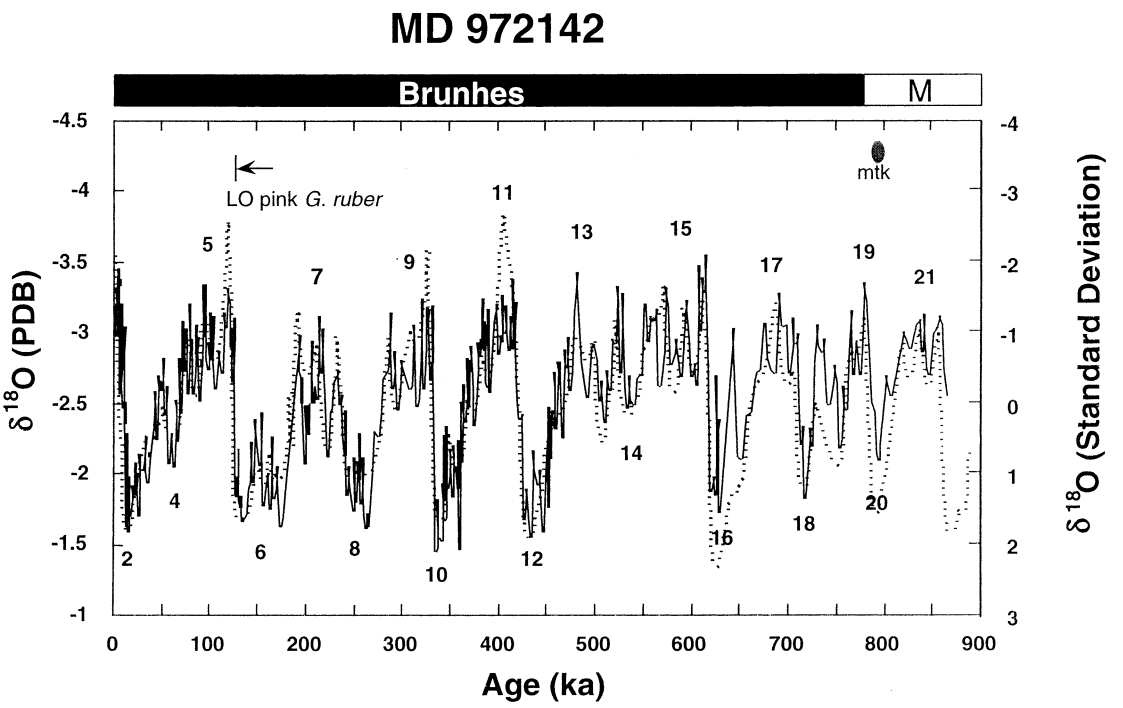

Fig. 3. Oxygen isotope timescale of *Globigerinoides ruber*, Core MD972142, calibrated against the low-latitude oxygen isotope stack of Bassinot et al. (1994) (shown as the dotted line). The scale for the MD972142 $\delta^{18}O$ is shown on the left axis while that for the low-latitude stack is on the right axis. Shown on the top are the magnetic polarity from Lee (2000), the last occurrence datum of pink *G. ruber*, and the interval of Australasian microtektites (marked as mtk) (Lee and Wei, 2000). The final fixpoints for the timescale are listed in Table 1.

4. Oxygen isotope stratigraphy

Results of the oxygen stable isotope measurements are plotted in Fig. 2. The profile shows a fluctuation pattern comparable to previously published records of the late Quaternary in the low-latitude Pacific (e.g. V28-238 by Shackleton and Opdyke, 1973 and DSDP 805C by Berger et al., 1993a on Ontong Java Plateau; ODP 769 in Sulu Sea by Linsley and Dunbar, 1994). The Brunhes/Matuyama geomagnetic reversal at 33.70 m (Lee, 2000) assists in positioning the marine isotopic stages 19 and 20. The occurrence of Australasian microtektites at the subdepths 33.85–34.45 m further constrains the age of this interval to be ~770–790 ka (Izett and Obradovich, 1992; Tauxe et al., 1996; Lee and Wei, 2000). These biostratigraphic, magnetostratigraphic and microtektite markers were used as independent controls in assisting the correlation of the resulted profile with the low-latitude stack (Bassinot et al., 1994) (Fig. 3). The depths and corresponding ages of the controlling points are listed in Table 1. The newly calibrated ages of the various independent markers are listed, too.

Compared to the typical glacial–interglacial difference of ~1.4‰ in $\delta^{18}O$ observed in open-ocean records of the Ontong Java Plateau (Shackleton and Opdyke, 1973; 1976; Berger et al., 1993a,b), the amplitude of fluctuation as large as ~2‰ for the glacial–interglacial cycles in MD972142 is significantly larger. This amplified $\delta^{18}O$ variation observed in this core is considered to be an ensemble effect of global ice-volume variation and local temperature and salinity changes. The semi-isolated configuration of the SCS Basin during periods of low sea-level stand together with the changing salt budgets (varying intensities

Table 1
Chronological delineators in MD972142

Depth (cm)	Age (ka)	Method
1	1	AMS ^{14}C
69	5	AMS ^{14}C
145	6	
201	12	AMS ^{14}C
225	14	AMS ^{14}C
241	16	
297	21	AMS ^{14}C
425	34	
601	52	MIS 3.1
675	64	
747	80	MIS 5.1
813	94	
865	106	MIS 5.4
893	122	MIS 5.5
929	128	MIS 6.0
995	136	
1034	148	
1056	156	
1104	166	
1140	176	
1172	194	MIS 7.1
1347	214	MIS 7.3
1379	224	MIS 7.4
1419	234	
1493	250	
1589	266	MIS 8.4
1663	288	MIS 8.5
1705	296	MIS 8.6
1778	316	MIS 9.2
1838	328	MIS 9.3
1896	342	
1924	348	MIS 10.3
1974	358	
2042	370	MIS 11.1
2090	384	MIS 11.23
2126	392	
2221	420	
2256	434	MIS 12.2
2284	452	
2425	482	MIS 13.11
2441	492	MIS 13.12
2457	500	MIS 13.13
2489	510	MIS 13.2
2529	524	MIS 13.3
2589	536	MIS 14.2
2713	574	MIS 15.1
2777	596	
2809	604	MIS15.4
2857	616	MIS 15.5
2881	624	
2921	630	
2929	644	
2961	662	
3033	690	
3073	702	
3121	710	
3153	718	MIS 18.2
3193	730	MIS 18.3
3265	754	MIS 18.4
3329	766	MIS 19.1
3385	780	
3417	792	MIS 20.2
3449	796	
3465	808	
3473	820	MIS 21.1
3489	828	MIS 21.2
3505	838	MIS 21.3
3537	848	MIS 21.4
3561	858	MIS 21.5
*910	125	LA of pink *Globigerinoides ruber*
*3370	776	Brunhes/Matuyama boundary
*3425	793	Australasian microtektite peak

of terrestrial freshwater runoff and exchange efficacy with open-ocean saline waters) should have contributed to amplifying the $\delta^{18}O$ variation.

To enable a comparison of the oxygen isotope time-series of MD972142 with the isotopic profile yielded from the same species from Site ODP769 at 8°N latitude in the Sulu Sea (Linsley and Dunbar, 1994; Linsley, 1996), we calibrated the ODP769 record to the timescale of MD972142 by curve matching. The curve matching was conducted using the AnalySeries Program, Version 1.2. (Paillard et al., 1996).

5. Maritime proxy of the East Asia summer monsoons

The calibration of the $\delta^{18}O$ profile of ODP769 against the timescale of MD972142 allows a close comparison of the two time-series (Fig. 4A). Given the fact that both sites (MD 972142 in the SCS and ODP 769 in the Sulu Sea) are located in the northwest margin of the West Pacific Warm Pool (WPWP) with similar latitudes, the oxygen iso-

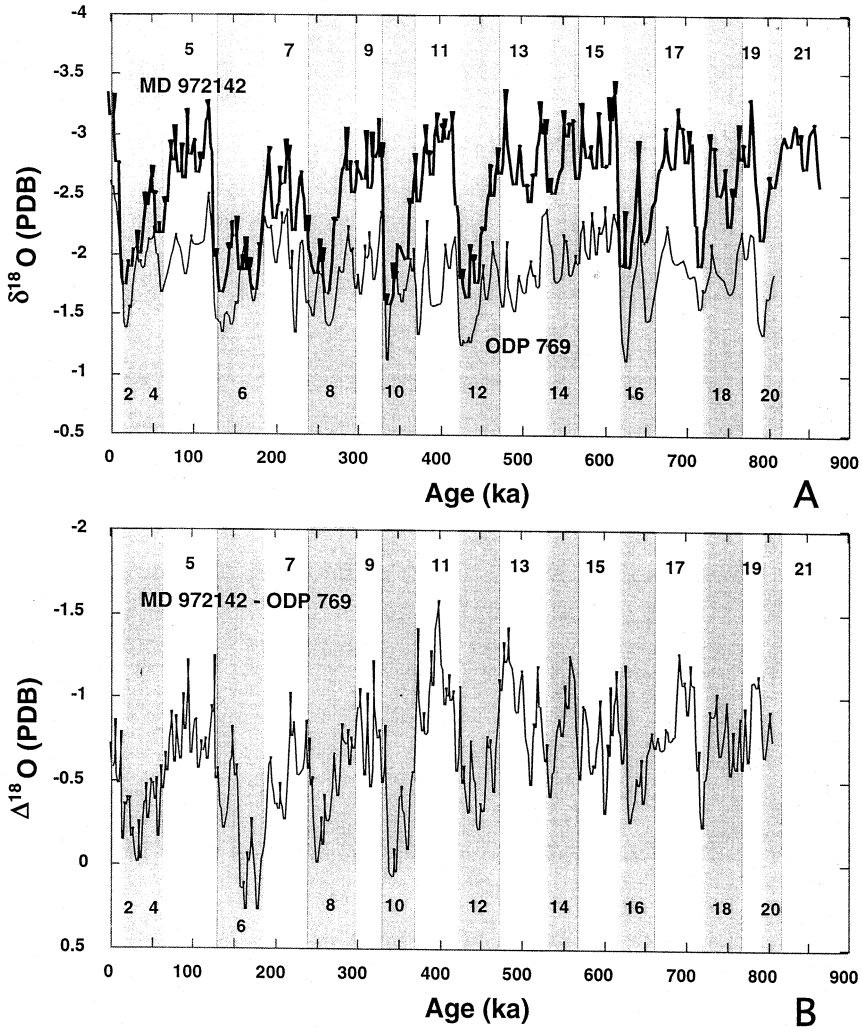

Fig. 4. Comparison of oxygen isotope profile of MD972142 with that of ODP769 of the Sulu Sea. Marine oxygen isotopic stages down to stage 21 are marked. Glacial stages are represented by gray stripes. (A) Time-series of $\delta^{18}O$ of both sites with a time interval of 2k ($\Delta t = 2k$) of both sites are interpolated from the original data profiles and shown here. MD972142 shows lower $\delta^{18}O$ values during most of the last 800 kyr. (B) The $\delta^{18}O$ difference between the interpolated time-series of MD972142 and ODP769 calculated by subtracting the values of ODP769 from that of MD972142. The depletion of ^{18}O is more distinctive during the interglacial periods.

topic values obtained from the same species of planktic foraminiferal tests are expected to be the same, or at least, similar. Yet, MD972142 tends to show more negative $\delta^{18}O$ values than ODP769, especially during the interglacial stages (the odd-numbered stages in Fig. 4). The difference in $\delta^{18}O$ between the two sites decreases during the glacial periods but increases during interglacial intervals (Fig. 4B). Larger gradients ($\delta^{18}O_{MD142}$–$\delta^{18}O_{ODP769}$) up to 0.5–1.5‰ exist for most parts of the interglacial stages but with small differences of 0–0.5‰ during the glacial stages (Fig. 4B). This result is somewhat counter-intuitive in that the two basins should be more isolated from each other during glacial periods when sea level dropped, therefore showing

different values. On the other hand, there should be more water exchange between these two basins during interglacial periods when the sea levels were higher.

Over the late Quaternary, such systematic discrepancies must result from a significant difference in temperature or salinity, or a combination of both, of the surface waters of these two basins. Furthermore, the amplitude of the fluctuation in MD972142 time-series also is larger, attesting an amplified effect of the SCS. At present, the sea-surface temperatures (SSTs) of these two basins are quite similar (Levitus and Boyer, 1994). The difference in temperature during the past could be due to the shifting of the western extent of the WPWP (Martinez et al., 1997). On the other hand, the salinity of the Sulu Sea surface water at present is slightly higher than that in the SCS by 0.5‰ (Levitus et al., 1994).

Although the foraminifera used by both studies were well preserved, and the inter-laboratory difference in oxygen isotopic measurements was evaluated to be small (pers. commun. Linsley, 1998), we could not absolutely rule out the possibility that there exists a systematic difference in $\delta^{18}O$ values between these two time-series introduced by experimental practice. To further check if the observed difference is not merely an artifact, we normalized each time-series to its own average value, and calculated the gradient between these two normalized time-series again (Fig. 5B). The result yields an almost identical pattern with Fig. 4B.

Such an ever-lasting difference in $\delta^{18}O$ between the SCS and Sulu Sea must result from a significant difference in hydrographic condition between the two basins during the past 800 kyr. The relatively more negative $\delta^{18}O$ values in MD972142 can only be accounted for by higher temperature or lower salinity, or a combination of both. However, the former factor – higher SSTs in the SCS – is less likely because the Sulu Sea is located closer to the core of the WPWP and is warmer. The glacial–interglacial SST difference in the core WPWP was about 1–3°C (CLIMAP, 1981; Ohkouchi et al., 1994; Lea et al., 2000). In contrast, SSTs in the SCS dropped by as much as 3–6°C (L. Wang and Wang, 1990; Miao et al., 1994; Thunell et al., 1995; Chen and Huang, 1998; Wei et al., 1998a; Pelejero et al., 1999; L. Wang et al., 1999; Kienast et al., 2001) (equivalent to ~0.75–1.5‰ increase in $\delta^{18}O$ signal) from the interglacial to glacial intervals. The SSTs seldom exceeded the modern temperature in the past. For instance, the increase in SST (reconstructed by alkenone insaturation index) during the warmest period, substage 5.5 (~125 ka) in the last interglacial, was less than 1°C than the Holocene (P. Wang et al., 1999). Therefore, temperature variation (mostly becoming colder) alone in the SCS would likely have caused the $\delta^{18}O$ values to be more positive relative to the Sulu Sea, opposite to the observed negative tendency. One possible explanation for the light oxygen isotope composition of MD972142 is that over most part of the past 800 kyr, the $\delta^{18}O$ values of the surface waters of the SCS were lower than in the Sulu Sea, especially during the interglacial periods. Today, rivers in Indochina, Borneo and Sumatra serve as major sources of freshwater to the SCS, it is conceivable to assume that during the interglacial periods, enhanced precipitation and increased runoff would result in lower $\delta^{18}O$ values for surface waters particularly for the southern part of the SCS. And meanwhile, the Sulu Sea was more or less immune from the influence of the increased freshwater runoff. In fact, long-term observation of land and ocean precipitation of the studied area (the CAMS–OPI monthly precipitation climatology available from http://ingrid.ldgo.columbia.edu/) shows that starting from June to the end of October, when southwesterly monsoons are prevailing, the Indochina Peninsula and the SCS are under heavy precipitation. Particularly, the 'bull-eyes' of peak precipitation larger than 400 mm/month are located over the southern Indochina Peninsula and the eastern part of the SCS. In comparison, the precipitation over Sulu Sea is less than 300 mm/month.

Modern climate data suggest that the strongest convective precipitation in the SCS and over the Indochina Peninsula is associated with the Inter-Tropical Convergence Zone (ITCZ) (Lau and Li, 1984; Hoffman and Heimann, 1997); the position of the ITCZ, in turn, is controlled by the north–south thermal gradient through the troposphere.

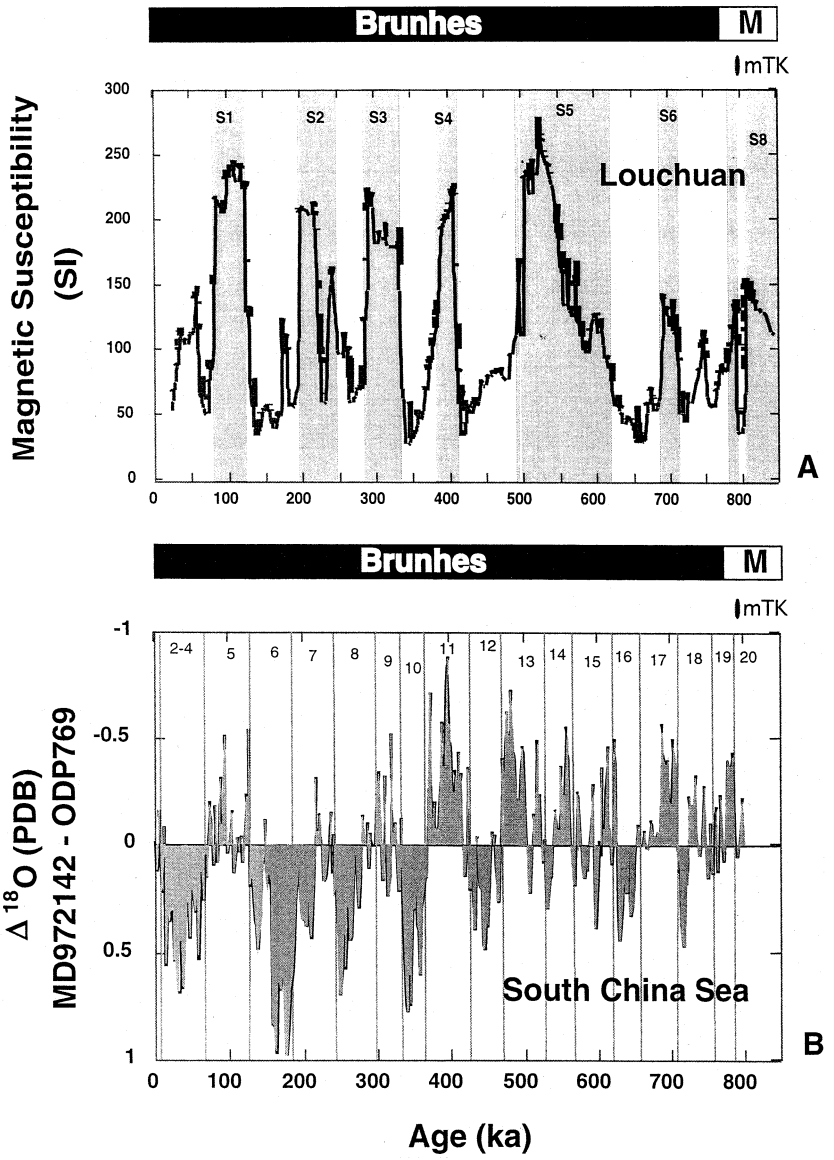

Fig. 5. Comparison of the terrestrial proxy of summer monsoons at Louchuan, Chinese Loess Plateau (A) with the maritime summer monsoon proxy (B). (A) Magnetic susceptibility of Louchuan Section in the central Chinese Loess Plateau, adopted from Heslop et al. (2000). Paleosol units (S1–S8) of the Louchuan Section are marked by light gray. (B) Maritime summer monsoon proxy of the SCS. The proxy is the difference in $\delta^{18}O$ between the average-normalized time-series of MD972142 and ODP769. Marine oxygen isotope stages down to stage 20 are marked. Magnetostratigraphy shown on top of each panel and the Australasian microtektite (mTK) layers at the three sites provided with independent chronological markers that support the correlation.

Furthermore, in convectively active regions such as the tropical islands and monsoon prevailing areas, the amount effect on $\delta^{18}O$ is significant (Dansgarrd, 1964). For instance, the $\delta^{18}O$ values drop from 0‰ to −7‰ when precipitation increases from 0 to 350 mm/month (Hoffman and Heimann, 1997). To demonstrate the link between the negative $\delta^{18}O$ values and the summer mon-

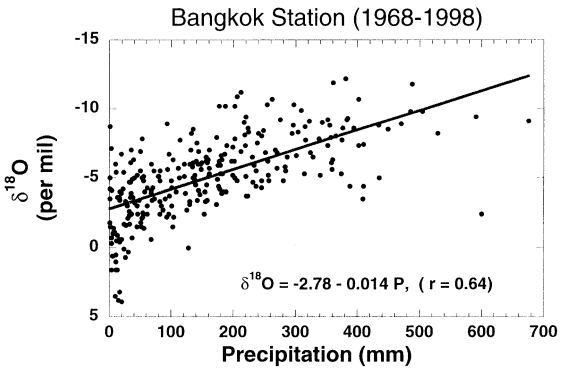

Fig. 6. Regression of $\delta^{18}O$ of precipitation against the monthly precipitation amount at the Bangkok Station over the period of 1968–1998. The linear relationship suggests the existence of an amount effect of precipitation on the $\delta^{18}O$ values of precipitation. The amount effect is estimated to be −1.4‰ per 100 mm precipitation. The data were obtained from the website of the Global Network for Isotopes in Precipitation, managed by the Isotope Hydrology Information System (http://isohis.iaea.org).

soons, we examined the precipitation data collected by IAEA at Bangkok for Year 1968–1998. The data show clearly that precipitation over these 30 years has been concentrated in the summer–early autumn and the $\delta^{18}O$ values dropped to as low as −12‰ when the monthly precipitation exceeded 500 mm. The amount effect was estimated as −1.4‰ per 100 mm/month increase in precipitation (Fig. 6).

Based upon the above reasoning, the negative excursion in $\delta^{18}O$ of Site MD972142 from that of ODP769 (Fig. 5B) can be regarded as an indication of excessive input of freshwater/precipitation to the SCS, and thus an indicator of summer monsoon intensity. The increased excursion ($\Delta^{18}O$ in Fig. 5B) during the interglacial periods is consistent with most previous inferences about the East Asian monsoon variation in the SCS, that the summer monsoon was stronger during the interglacial periods with a concomitant weakening of the winter monsoon (L. Wang and Wang, 1990; Huang et al., 1997; L. Wang et al., 1999; Jian et al., 2001). The variation pattern of this summer monsoon index (Fig. 5B) shows several important features: (1) precipitation (summer monsoon) was strengthened generally during the interglacial stages, and (2) the oxygen isotopic stage 14 is peculiar in showing heavy precipitation and strong summer monsoon, which is at odds with other glacial stages.

More strikingly, this 'maritime summer monsoon' index agrees very well with the magnetic susceptibility record of Louchuan, central Chinese Loess Plateau (Heslop et al., 2000) (Fig. 5A). The magnetic susceptibility of loess–paleosol sequences has long been regarded a proxy of summer monsoons over the Chinese Loess Plateau (An et al., 1990, 1991; Porter et al., 2001). The paleosol units are usually developed during the interglacial stages and characterized by high magnetic susceptibility. Here we adopted the astronomically tuned time scale of Heslop et al. (2000) to make a comparison between the maritime and terrestrial proxies of the summer monsoons. The widespread Australasian microtektites caused by an asteroid impact on the Indochina Peninsula slightly before the Matuyama/Brunhes geomagnetic boundary serves as an independent age marker to line up the three records under scrutiny: the microtektites (symbolized as mTK in Fig. 5) were found within the oxygen isotope stage 20 in Core MD972142 (Lee and Wei, 2000) and ODP769 (Schnieder et al., 1992; Kent and Schneider, 1995), and within the loess unit L8 at the Louchuan section (Fig. 5) (Li et al., 1993, fide Zhou and Shackleton, 1999).

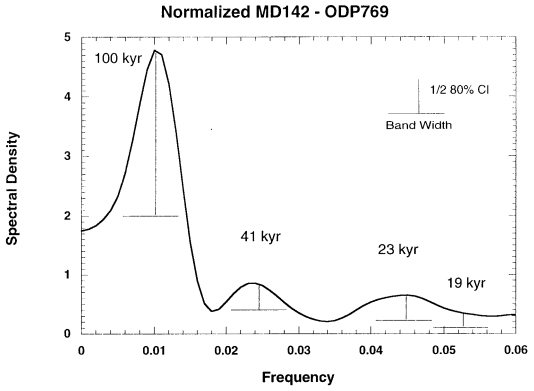

Fig. 7. Power spectra of maritime summer monsoon proxy of the South China Sea for the last 800 kyr. The vertical bar represents half of the 80% confidence interval whereas the horizontal bar is the bandwidth of the spectral analysis. Note that the time-series is dominated by the periodicity of eccentricity of 100 kyr.

Generally speaking, high values of magnetic susceptibility shown by the Louchuan Section correspond to negative excursions shown by the maritime proxy (Fig. 5). For a long time it has been perplexing that the thickest paleosol unit (S5) spans across a prolonged period of marine oxygen isotope stages 15–13 (MIS 15–13). Here the $\Delta^{18}O$ shows large negative values over most of MIS 15–13, suggesting that the intensified summer monsoons might not only have caused high precipitation over Southeast Asia and the SCS, but also induced warm and wet conditions over the Chinese Loess Plateau in this particular period (Fig. 5). Similarly, the paleosol unit S3 also extends into the first half of MIS 8 where the summer monsoons were intensified (Fig. 5). Paleosol unit S1 also finds its counterpart during MIS 5 in the maritime index. The only interval where the maritime index does not correspond well is in the second half of MIS 7 where the low $\Delta^{18}O$ gradient does not match well with the high SI values of the loess. But, on the other hand, the peak SI values in the early part, namely those during 650–850 ka, match quite well with high $\Delta^{18}O$ values in their counterparts, respectively (Fig. 5). A spectral analysis of the maritime summer monsoon index reveals that the time-series is dominated by the 100-kyr periodicity of eccentricity (Fig. 7). The explanation power of this newly established maritime proxy appears to merit it a faithful indicator of the Asian summer monsoon intensity at least at the glacial–interglacial time scale. The MD972142 oxygen isotope profile indicates that the western margin of the WPWP over the southeastern SCS has been highly variable, partially contributed by the changing intensities of summer monsoons at the glacial–interglacial time-scale.

6. Summary

The late Quaternary planktic foraminiferal $\delta^{18}O$ record obtained from Core MD972142 (12°41.33′N, 119°27.90′E; 1557 m water depth) of eastern South China was correlated with the astronomically tuned low-latitude stack of Bassinot et al. (1994). The $\delta^{18}O$ values at Site MD972142 are always lighter than those recorded at Site ODP 769 of the neighboring Sulu Sea, suggesting the existence of lower salinities in the SCS. The fluctuation amplitudes in $\delta^{18}O$ between the glacial and interglacial periods are also much larger than those of the Sulu Sea (ODP 769) by showing more negative values during the interglacial periods. We interpret this phenomenon as caused by enhanced precipitation over Indochina, Sumatra and Borneo during interglacial periods. The difference in $\delta^{18}O$ between the average-normalized $\delta^{18}O$ time-series of the SCS (MD972142) and the Sulu Sea (ODP769) is considered to be a maritime proxy of the East Asia summer monsoons. This maritime proxy shows good correlation with the summer monsoon index obtained from the Louchuan Section of central Chinese Loess Plateau. Notably, high values of maritime summer monsoon index during MIS 9–8.5 (340–280 ka) and MIS 15–13 (620–480 ka) can account for the prolonged development of thick paleosols of S3 and S5, respectively. The amplified planktic $\delta^{18}O$ signals of the SCS relative to the Sulu Sea record are partly caused by the changing intensities of the East Asian monsoons at the glacial–interglacial time-scale throughout the late Quaternary.

Acknowledgements

This study is a contribution to the Taiwan IMAGES Program and the APEC Project. Special thanks are extended to Drs. Min-Te Chen and Bernhard Diekmann for their instructions on conducting the time-series analyses presented. We thank the scientific party and crew of IMAGES-III-IPHIS-Leg II Cruise for a successful coring in the SCS. The support offered by French MENRT, TAFF, CNRS/INSU and IFRTP to the operation of the cruise vessel *Marion Dufrense* and the IMAGES Program is highly appreciated. We thank Dr. Brad Linsley for providing us his ODP 769 data and his laboratory standards. Dr. Heslop kindly provided the calibrated magnetic susceptibility data of the Louchuan Section. This study has been supported by Grants NSC-88-2116-002-012 and NSC-90-2166-M002-019 to K.-Y.W. and Y.-G.C. For curation of cores and

sampling service, we acknowledge the Core Laboratory located at the National Taiwan Ocean University, funded by the Center for Ocean Research, National Science Council, Taiwan.

References

An, Z.S., Kukla, G.J., Porter, S.C., Xiao, J.L., 1991. Magnetic susceptibility evidence of monsoon variation of the Loess Plateau of central China during the last 130,000 years. Quat. Res. 36, 29–36.

An, Z.S., Liu, T.S., Lu, Y.C., Porter, S.C., Kukla, G.J., Wu, X.H., Hua, Y.M., 1990. The long-term paleomonsoon variation recorded by the loess-paleosol sequence in central China. Quat. Int. 7/8, 91–95.

Bassinot, F.C., Labeyrie, L.D., Vincent, E., Quidelleur, X., Shackleton, N.J., Lancelot, Y., 1994. The astronomical theory of climate and the age of the Brunhes–Matuyama magnetic reversal. Earth Planet. Sci. Lett. 126, 91–108.

Berger, W.H., Bickert, T., Schmidt, H., Wefer, G., Yasuda, M., 1993a. Quaternary oxygen isotope record of pelagic foraminifers: Site 805, Ontong Java Plateau. In: Berger, W.H., Kroenke, L.W., Mayer, L.A., et al. (Eds.), Proc. ODP, Sci. Results 130, Ocean Drilling Program, College Station, TX, pp. 363–379.

Berger, W.H., Bickert, T., Schmidt, H., Wefer, G., 1993b. Quaternary oxygen isotope record of pelagic foraminifers: Site 806, Ontong Java Plateau. In: Berger, W.H., Kroenke, L.W., Mayer, L.A., et al. (Eds.), Proc. ODP, Sci. Results 130, Ocean Drilling Program, College Station, TX, pp. 381–395.

Brummer, G.-J.A., Hemleben, C., Spindler, M., 1987. Ontogeny of extant spinose planktonic foraminifera (Globigerinidae): A concept exemplified by *Globigerinoides sacculifer* (Brady) and *G. ruber* (D'Orbigny). Mar. Micropaleontol. 12, 357–381.

Chen, C.-T.A., Huang, M.-H., 1996. A mid-depth front separating the South China Sea Water and the Philippine Sea Water. J. Oceanogr. 52, 17–25.

Chen, M-T., Beaufort, L., 1998. Exploring Quaternary variability of the East Asian monsoon. Kuroshio Current, and the Western Pacific warm pool systems: high-resolution investigations of paleoceanography from the IMAGES III/MD106 – IPHIS cruise TAO. Terr. Atmos. Ocean. Sci. 9, 129–142.

Chen, M.-T., Huang, C.-Y., 1998. Ice-volume forcing of winter monsoon climate in the South China Sea. Paleoceanography 13, 622–633.

CLIMAP, 1981. Seasonal reconstructions of the Earth's surface at the Last Glacial Maximum. Map and Chart Series MC-36, Geological Society of America.

Dansgarrd, W., 1964. Stable isotopes in precipitation. Tellus 16, 436–468.

Ding, Z.L., Liu, T.S., Rutter, N.W., Yu, Z.W., Guo, Z.T., Zhu, R.X., 1995. Ice-volume forcing of East Asian winter monsoon variation in the past 800,000 years. Quat. Res. 44, 140–159.

Gong, G.-C., Liu, K.-K., Liu, C.-T., Pai, S.-C., 1993. The chemical hydrography of the South China Sea west of Luzon and a comparison with the West Philippine Sea. Terr. Atmos. Ocean. Sci. 3, 587–602.

Heslop, D., Langereis, C.G., Dekkers, M.J., 2000. A new astronomical timescale for the loess deposits of Northern China. Earth Planet. Sci. Lett. 184, 125–139.

Hoffman, G., Heimann, M., 1997. Water isotope modeling in the Asian monsoon region. Quat. Int. 37, 115–128.

Huang, C.-Y., Liew, P.-M., Zhao, M., Chang, T.-C., Kuo, C.-M., Chen, M.-T., Wang, C.-H., Zheng, L.-F., 1997. Deep sea and lake records of the southeast Asian paleomonsoons for the last 35 thousand years. Earth Planet. Sci. Lett. 146, 59–72.

Izett, G.A., Obradovich, J.D., 1992. Laser-fusion $^{40}Ar/^{39}Ar$ ages of Australasian tektites (abstract). Lunar Planet. Sci. 23, 593–594.

Jian, Z., Huang, B., Kuhnt, W., Lin, H.-L., 2001. Late Quaternary upwelling intensity and East Asian monsoon forcing in the South China Sea. Quat. Res. 55, 363–370.

Kent, D.V., Schneider, D.A., 1995. Correlation of paleointensity variation records in the Brunhes/Matuyama polarity transition interval. Earth Planet. Sci. Lett. 129, 135–144.

Kienast, M., Steinke, S., Stattegger, K., Calvert, S.E., 2001. Synchronous tropical South China Sea SST change and Greenland warming during deglaciation. Science 291, 2132–2134.

Lau, K.-M., Li, T., 1984. The monsoon of East Asia and its global associations – a survey. Bull. Am. Meteorol. Soc. 65, 114–125.

Lea, D.W., Pak, D.K., Spero, H., 2000. Climate impact of late Quaternary equatorial Pacific sea surface temperature variation. Science 289, 1719–1724.

Lee, M.-Y., Wei, K.-Y., 2000. Australasian microtektites in the South China Sea and the West Philippine Sea: Implications for age, size and location of the impact crater. Meteorit. Planet. Sci. 35, 1151–1155.

Lee, M.-Y., Wei, K.-Y., Chen, Y.-G., 1999. High resolution oxygen isotope stratigraphy for the last 150,000 years in the southern South China Sea: core MD972151. Terr. Atmos. Ocean. Sci. 10, 239–254.

Lee, T.-Q., 2000. Geomagnetic secular variation of the last one million years recorded on core MD972142 from the southeast South China Sea. J. Geol. Soc. China 43, 423–433.

Levitus, S., Boyer, T.P., 1994. World Ocean Atlas, Vol. 4, Temperature. NOAA, U.S. Dept. Commerce, Washington, DC.

Levitus, S., Burgett, R., Boyer, T.P., 1994. World Ocean Atlas, Vol. 3, Salinity. NOAA, U.S. Dept. Commerce, Washington, DC.

Li, C.L., Ouyang, Z.Y., Liu, T.S., An, Z.S., 1993. Microtektites and glassy microspherules in loess – their discoveries and implication. Sci. China B36, 1141–1152.

Linsley, B.K., 1996. Oxygen-isotope record of sea level and climatic variation in the Sulu Sea over the past 150,000 years. Nature 380, 234–237.

Linsley, B.K., Dunbar, R.B., 1994. The late Pleistocene history of surface water $\delta^{13}C$ in the Sulu Sea: Possible relationship to Pacific deepwater $\delta^{13}C$ changes. Paleoceanography 9, 317–340.

Lu, H., Liu, X., Zhang, F., An, Z., Dodson, J., 1999. Astronomical calibration of loess–paleosol deposits at Louchuan, central Chinese Loess Plateau. Palaeogeogr. Palaeoclimatol. Palaeoecol. 154, 237–246.

Martinez, J.I., DeDeckker, P.D., Chivas, A.R., 1997. New estimates for salinity changes in the Western Pacific Warm Pool during the Last Glacial Maximum: Oxygen-isotope evidence. Mar. Micropaleontol. 32, 311–340.

Miao, Q., Thunell, R.C., Anderson, D.M., 1994. Glacial–Holocene carbonate dissolution and sea surface temperature in the South China and Sulu Seas. Paleoceanography 9, 269–290.

Nitani, H., 1972. Beginning of the Kuroshio. In: Stommel, H., Yoshida, K. (Eds.), Kuroshio. University of Washington Press, pp. 129–163.

Ohkouchi, N., Kawamura, T., Nakamura, T., Taira, A., 1994. Small changes in the sea surface temperature during the last 20,000 years: Molecular evidence from the western tropical Pacific. Geophys. Res. Lett. 21, 2207–2210.

Paillard, D., Labeyrie, L., Yiou, P., 1996. Macintosh program performs time-series analysis. EOS Trans. AGU 77, 379.

Pelejero, C., Grimalt, J.O., Sarnthein, M., Wang, L., Flores, J.-A., 1999. Molecular biomarker record of sea surface temperature and climatic change in the South China Sea during the last 140,000 years. Mar. Geol. 156, 109–121.

Porter, S.C., Hallet, B., Wu, X., An, Z., 2001. Dependence of near-surface magnetic susceptibility on dust accumulation rate and precipitation on the Chinese Loess Plateau. Quat. Res. 55, 271–283.

Prell, W.L., Marvil, R.E., Luther, M.E., 1990. Variability in upwelling fields in the Northwestern Indian Ocean – 2. Data-model comparison at 9000 years B.P.. Paleoceanography 5, 447–457.

Rottman, M.L., 1979. Dissolution of planktonic Foraminifera and pteropods in the South China Sea sediments. J. Foraminif. Res. 9, 41–49.

Schneider, D.A., Kent, D.V., Mello, G.A., 1992. A detailed chronology of the Australasian impact event, the Brunhes–Matuyama geomagnetic polarity reversal, and global climate change. Earth Planet. Sci. Lett. 111, 395–405.

Shackleton, N.J., Opdyke, N.D., 1973. Oxygen isotope and paleomagnetic stratigraphy of equatorial Pacific Core V28-238: Oxygen isotope temperatures and ice volumes on a 10^5 year and 10^6 year scale. Quat. Res. 3, 39–55.

Shackleton, N.J., Opdyke, N.D., 1976. Oxygen isotope and paleomagnetic stratigraphy of equatorial Pacific Core V28-239: Late Pliocene to latest Pleistocene. In: Cline, R., Hays, J.D. (Eds.), Investigation of Late Quaternary Paleoceanography and Paleoclimatology. Mem. Geol. Soc. Am. 145, pp. 449–464.

Shaw, P.-T., 1989. The intrusion of water masses into the sea southwest of Taiwan. J. Geophys. Res. 94, 18213–18226.

Shaw, P.-T., 1991. The seasonal variation of the intrusion of the Philippine Sea water into the South China Sea. J. Geophys. Res. 96, 821–827.

Sun, X., Li, X., 1999. A pollen record of the last 37 ka in deep sea core 17940 from the northern slope of the South China Sea. Mar. Geol. 156, 227–242.

Tauxe, L., Herbert, T., Shackleton, N.J., Kok, Y.-S., 1996. Astronomical calibration of the Matuyama–Brunhes boundary: Consequences for magnetic remanence acquisition in marine carbonates and the Asian loess sequences. Earth Planet. Sci. Lett. 140, 133–146.

Thompson, P.R., Bé, A.W.H., Duplessy, J.-C., Shackleton, N.J., 1979. Disappearance of pink-pigmented *Globigerinoides ruber* at 120,000 yr BP in the Indian and Pacific Oceans. Nature 280, 554–558.

Thunell, R.C., Anderson, D., Gellar, D., Miao, Q.M., 1995. Sea-surface temperature estimates for the tropical western Pacific during the last glaciation and their implications for the Pacific warm pool. Quat. Res. 41, 255–264.

Verosub, K.L., Fine, P., Singer, M.J., TenPas, J., 1993. Pedogenesis and paleoclimate: Interpretation of the magnetic susceptibility record of Chinese loess–paleosol sequences. Geology 21, 1011–1014.

Wang, L., Wang, P., 1990. Late Quaternary paleoceanography of the South China Sea: Glacial–interglacial contrasts in as enclosed basin. Paleoceanography 5, 77–90.

Wang, L., Sarnthein, M., Erlenkeuser, H., Grimalt, J., Groote, P., Heiling, S., Ivanova, E., Kienast, M., Pelejero, C., Pflaumann, U., 1999. East Asian monsoon climate during the late Pleistocene: High-resolution sediment records from the South China Sea. Mar. Geol. 156, 245–284.

Wang, P., 1999. Response of western Pacific marginal seas to glacial cycles: Paleoceanographic and sedimentological features. Mar. Geol. 156, 5–39.

Webster, P.J., Yang, S., 1992. Monsoon and ENSO: Selectively interactive system. Quat. J. R. Met. Soc. 118, 877–926.

Wei, K.-Y., Lee, M.-Y., Duan, W., Chen, C., Wang, C.-H., 1998a. Paleoceanographic change in the northeastern South China Sea during the last 15,000 years. J. Quat. Sci. 13, 55–64.

Wei, K.-Y., Lee, T.-Q., and Shipboard Scientific Party of IMAGES III/MD106-IPHIS Cruise (Leg III), 1998b. Late Pleistocene volcanic ash layers in Core MD972142, offshore of Northwestern Palawan, South China Sea: A preliminary report. Terr. Atmos. Ocean. Sci. 9, 143–152.

Wei, K.-Y., Zhang, Z.-W., Wray, C., 1992. Shell ontogeny of *Globorotalia inflata* (I): Growth dynamics and ontogenetic stages. J. Foraminif. Res. 22, 318–327.

Wytrki, K., 1961. Physical oceanography of the Southeast Asian Waters. In: NAGA Report, Vol. 2, Scripps Inst. of Oceanography, La Jolla, CA, 195 pp.

Zhou, L.P., Shackleton, N.J., 1999. Misleading positions of geomagnetic reversal boundaries in Eurasian loess and implications for correlation between continental and marine sedimentary sequences. Earth Planet. Sci. Lett. 168, 117–130.